processes

MDPI

Article

Hybrid MBR–NF Treatment of Landfill Leachate and ANN-Based Effluent Prediction

Ender Çetin [1], Vahit Balahorlu [2] and Sevgi Güneş-Durak [3,*]

[1] Department of Environmental Engineering, Faculty of Engineering, Istanbul University-Cerrahpaşa, Avcılar 34320, Istanbul, Türkiye; ecetin@iuc.edu.tr
[2] IZAYDAS, Izmit 41000, Kocaeli, Türkiye; balahorli@gmail.com
[3] Department of Environmental Engineering, Faculty of Engineering-Architecture, Nevsehir Haci Bektas Veli University, Nevsehir 50300, Nevsehir, Türkiye
* Correspondence: sgdurak@nevsehir.edu.tr

Abstract: This study presents the long-term performance evaluation of a full-scale hybrid membrane bioreactor (MBR)–nanofiltration (NF) system for the treatment of high-strength municipal landfill leachate from the Istanbul–Şile Kömürcüoda facility. Over a 16-month operational period, influent and effluent samples were analyzed for key parameters, including chemical oxygen demand (COD), ammonium nitrogen (NH_4^+-N), total phosphorus (TP), suspended solids (SS), and temperature. The MBR unit consistently achieved high removal efficiencies for COD and NH_4^+-N (93.5% and 98.6%, respectively), while the NF stage provided effective polishing, particularly for phosphorus, maintaining a TP removal above 95%. Seasonal analysis revealed that the biological performance peaked during spring, likely due to optimal microbial conditions. To support intelligent control strategies, artificial neural network (ANN) models were developed to predict effluent COD and NH_4^+-N concentrations using influent and operational parameters. The best-performing ANN models achieved R^2 values of 0.861 and 0.796, respectively. The model's robustness was validated through RMSE, MAE, and 95% confidence intervals. Additionally, Principal Component Analysis (PCA) and Random Forest algorithms were employed to determine the parameter importance and nonlinear interactions. The findings demonstrate that the integration of hybrid membrane systems with AI-based modeling can enhance treatment efficiency and forecasting capabilities for landfill leachate management, offering a resilient and data-driven approach to sustainable operation.

Keywords: landfill leachate; membrane bioreactor (MBR); nanofiltration (NF); artificial neural network (ANN); COD removal; ammonium removal; effluent prediction

check for updates

Academic Editors: Md. Salatul Islam Mozumder, Rajan Kumar Thapa, Surajbhan Sevda and Nabin Aryal

Received: 7 May 2025
Revised: 31 May 2025
Accepted: 2 June 2025
Published: 4 June 2025

Citation: Çetin, E.; Balahorlu, V.; Güneş-Durak, S. Hybrid MBR–NF Treatment of Landfill Leachate and ANN-Based Effluent Prediction. *Processes* **2025**, *13*, 1776. https://doi.org/10.3390/pr13061776

Copyright: © 2025 by the authors. Licensee MDPI, Basel, Switzerland. This article is an open access article distributed under the terms and conditions of the Creative Commons Attribution (CC BY) license (https://creativecommons.org/licenses/by/4.0/).

1. Introduction

Landfill leachate is a highly variable and pollutant-rich wastewater stream generated as precipitation percolates through layers of solid waste. It typically contains elevated concentrations of organic matter, ammonium, heavy metals, salts, and persistent organic pollutants, posing significant risks to both surface and groundwater resources [1,2]. The chemical and biological characteristics of leachate are strongly influenced by factors such as the landfill age, waste composition, climatic conditions, and operational practices [3,4].

Although a range of conventional biological, chemical, and physical processes have been employed in leachate treatment, these conventional methods often fail to comply with increasingly stringent discharge regulations, especially regarding nitrogenous compounds and recalcitrant organics [5–7]. These limitations are especially pronounced in leachate from

large-scale urban landfills, where the persistence and toxicity of contaminants necessitate advanced treatment solutions. Moreover, fluctuating influent characteristics and process instability heighten the environmental risks due to the operator-dependent nature of traditional systems. Therefore, the development and deployment of more stable, modular, and intelligent technologies have become critical—not only for regulatory compliance but also for long-term environmental sustainability.

Among such technologies, membrane-based systems have emerged as highly effective solutions due to their compact design and capacity to produce high-quality effluent. The Membrane Bioreactor (MBR), in particular, integrates biological degradation with membrane separation, achieving the superior removal of organic pollutants while minimizing sludge production [8,9]. Recent studies underscore the robustness of MBR systems under variable leachate conditions. For example, Brancato et al. (2023) reported that intelligent bioreactors with learning-based control systems maintained microbial stability over extended operations [10].

In parallel, nanofiltration (NF) technologies have been developed to address specific separation challenges, including the removal of dissolved solids, multivalent ions, and low-molecular-weight organics. Liu et al. (2025) demonstrated that membrane surface charge plays a crucial role in determining the rejection efficiency for complex landfill leachates, enabling membrane tailoring to site-specific needs [11]. Similarly, Molina et al. (2024) emphasized the environmental monitoring potential of membrane-integrated Artificial Intelligence (AI) systems for illegal landfill identification [12]. Furthermore, NF serves as an efficient polishing step when combined with MBR, enhancing effluent quality while mitigating energy demand and membrane fouling [13,14]. For instance, Liu et al. (2023) achieved organic and salt recovery rates of 95.5% and 86.5%, respectively, by coupling loose NF with membrane distillation [15]. Similarly, Kim et al. (2024) showed that integrating MBR, NF, and reverse osmosis (RO) can significantly improve the effluent quality and water reuse potential [16].

AI-based modeling, particularly using Artificial Neural Networks (ANNs), has gained momentum in leachate treatment research. These tools offer significant advantages in terms of performance prediction, parameter optimization, and reducing the experimental workload. Rall et al. (2020) integrated ANN into multi-scale membrane design models, connecting nanoscale behavior with process economics [17]. Ling and Battiato (2019) further contributed by introducing a dynamic model that couples fluid flow, solute transport, and adsorption, leading to a universal scaling law useful for pressure-driven systems like RO and NF [18]. Numerous studies have also demonstrated the utility of ANN in optimizing various treatment processes, including electrocoagulation (Igwegbe et al., 2024), solar-driven photocatalysis (Desai et al., 2020), and hybrid system control (Matovelle et al., 2023; Singa et al., 2023) [19–22].

This study investigates the advanced treatment of landfill leachate from the Istanbul–Şile Kömürcüoda Sanitary Landfill using a full-scale MBR–NF system. Over a 16-month period, the system was evaluated for key performance indicators such as COD, ammonium, phosphate, and suspended solids. Furthermore, an ANN model was developed using influent characteristics and operational parameters to predict the effluent COD and ammonium concentrations. This work provides both practical and modeling insights for optimizing hybrid membrane systems and stands out by combining long-term real-world operational data with AI-based forecasting for sustainable leachate management.

2. Materials and Methods

2.1. Study Site Description and Sampling

This study was conducted at the Kömürcüoda municipal solid waste landfill leachate treatment facility located in Istanbul, Turkey. The facility is located at 41.14803° N latitude and 29.37708° E longitude. The plant employs membrane-based tertiary treatment processes, including Ultrafiltration (UF) followed by NF, in a sequential setup. Leachate samples were collected at key stages of the treatment process: influent, after the MBR, and after the NF unit.

2.2. Operational and Analytical Data Collection

Daily operational data including the chemical oxygen demand (COD), ammonium (NH_4^+-N), temperature, total suspended solids (TSS), and mixed liquor suspended solids (MLSS) were collected over a 16-month period (January 2009–April 2010). These data were used to evaluate the system performance and serve as input for modeling studies.

The collected data were evaluated using a statistical analysis method and the results obtained were compared with similar studies in the literature [23]. The influent parameters of the leachate entering the treatment plant and the effluent parameters according to the design criteria are given in Tables 1 and 2. Table 1 presents the physicochemical characteristics of the influent wastewater utilized throughout the experimental study. The wastewater exhibits a high organic load, as evidenced by the elevated values of COD (20,000 ± 1000 mg/L) and Biochemical Oxygen Demand over 5 days (BOD_5) (13,000 ± 800 mg/L), indicating the presence of readily biodegradable and persistent organic matter. Nitrogen pollution is also significant, with the Total Kjeldahl Nitrogen (TKN) levels reaching 3000 ± 200 mg/L, while the Total Phosphorus (TP) concentration (5 ± 0.3 mg/L) contributes to the nutrient load and potential risk of eutrophication. The sample is moderately acidic to neutral (pH range: 5.5–8.5), and its temperature is maintained at 20 ± 0.5 °C to ensure biological activity. The sulfate (SO_4^-) concentration (500 ± 25 mg/L) may influence microbial processes such as sulfate reduction. TSS are measured at 1500 ± 100 mg/L, reflecting the particulate matter burden in the system. A very high conductivity (40,000 ± 2000 µmhos/cm) suggests the presence of significant dissolved ions, which is further supported by the elevated total hardness (2500 ± 150 mg $CaCO_3$/L). Alkalinity (13,000 ± 600 mg $CaCO_3$/L) indicates a substantial buffering capacity, which helps maintain pH stability during biological treatment processes. These values reflect a challenging wastewater matrix typical of high-strength industrial effluents, necessitating robust and adaptive treatment technologies.

Table 1. Characteristics of the influent wastewater.

Parameter	Unit	Value
Flow rate	m^3/day	1200 ± 50
Temperature	°C	20 ± 0.5
pH	-	5.5–8.5 (±0.1 per reading)
COD	mg/L	20,000 ± 1000
BOD_5	mg/L	13,000 ± 800
TKN	mg/L	3000 ± 200
Total Phosphorus	mg/L	5 ± 0.3
SO_4^-	mg/L	500 ± 25
TSS	mg/L	1500 ± 100
Total Hardness	mg $CaCO_3$/L	2500 ± 150
Conductivity	µmhos/cm	40,000 ± 2000
Alkalinity	mg $CaCO_3$/L	13,000 ± 600

Table 2 outlines the maximum allowable concentrations for key physicochemical parameters in the treated effluent, based on design and regulatory compliance targets. These criteria are essential for ensuring that the treated wastewater meets discharge limits, protects receiving environments, and complies with national and international environmental standards. The effluent temperature is maintained below 35 ± 0.5 °C to prevent thermal pollution and to support the viability of aquatic ecosystems. The pH range of 6.0–9.0 (±0.1) ensures that the treated water remains within a biologically acceptable range, minimizing the risk of chemical toxicity or microbial inhibition. COD and BOD_5 are limited to 125 ± 5 mg/L and 50 ± 3 mg/L, respectively. These values reflect the target for organic matter reduction, indicating an efficient biological treatment performance. Nitrogen-related parameters, including Total Nitrogen (TN; 400 ± 20 mg N/L) and Total Kjeldahl Nitrogen (TKN; 50 ± 3 mg N/L), are controlled to reduce nutrient pollution and the risk of eutrophication in natural waters. Similarly, Total Phosphorus (TP) is limited to 2 ± 0.1 mg P/L, reflecting stringent phosphorus removal requirements to protect surface water quality. The limit for TSS is set at 35 ± 2 mg/L, which ensures low levels of particulate matter in the effluent and helps maintain clarity and quality in the receiving water bodies. These effluent quality criteria form the benchmark for evaluating the treatment system's performance and ensure the sustainability of discharge practices.

Table 2. Effluent design criteria for wastewater treatment plant.

Parameter	Unit	Maximum
Temperature	°C	35 ± 0.5
pH	-	6.0–9.0 (±0.1 per reading)
COD	mg/L	125 ± 5
BOD_5	mg/L	50 ± 3
TN	mg N/L	400 ± 20
TKN	mg N/L	50 ± 3
TP	mg P/L	2 ± 0.1
TSS	mg/L	35 ± 2

2.3. Analytical Methods

Physical, chemical, and biological parameters were measured using standard methods in accordance with international guidelines. The performance of the membrane systems was assessed through several analytical approaches. First, the removal efficiency (%) for each parameter was calculated using Equation (1):

$$\text{Removal Efficiency} = ((\text{Influent} - \text{Effluent})/\text{Influent}) \times 100 \quad (1)$$

Descriptive statistics, including mean, median, standard deviation, minimum, and maximum values, were computed for COD and NH_4^+-N removal data. To assess temporal variability, time-series analyses were conducted, highlighting trends and fluctuations in removal efficiencies throughout the study period. Correlation matrices were also developed to explore the relationships among the influent, effluent, and removal concentrations for COD and NH_4^+-N. Furthermore, ordinary least squares (OLS) regression modeling was employed to investigate the dependence of removal efficiency on influent concentrations. Table 3 summarizes the methods applied for the analysis of all parameters measured at different stages, including the raw leachate, UF effluent, and NF effluent. Additionally, pH and temperature were continuously monitored across various treatment stages, such as the raw leachate stream, anoxic and aerobic units of the bioreactor, UF, and NF units. These parameters, especially temperature, were incorporated into the AI-based modeling, where temperature was identified as a significant input variable affecting COD and NH_4^+-N

removal. While pH was considered as an indirectly effective parameter, both as an input and output, biological monitoring also included the biomass activity and dissolved oxygen (DO) levels, the latter being particularly critical for evaluating the leachate treatment efficiency.

Table 3. Analysis methods.

Parameter	Method	Device/Test Kit	Manufacturer Country	Typical Error
Influent				
pH		Hach-Lange HQ40dPortable multimeter	Germany	±0.002
Temperature		Hach-Lange HQ40dPortable multimeter	Germany	±0.2 °C
TSS	Gravimetric Method	Standard Method ST 2540 D [24]	Germany	±5–10%
COD	Photometric Method	Hach Lange Test Kit Method COD 1000–10,000 mg/L (LCK 014)	Germany	±5–10%
NH_4^+-N	Photometric Method	Hach Lange Test Kit Method NH-N, 47–130 mg/L (LCK302)	Germany	±5–10%
TN	Photometric Method	Hach Lange Test Kit Method 20–100 mg/L (LCK 338)	Germany	±5–10%
Phosphate (PO_4-P)	Photometric Method	Hach Lange Test Kit Method 2–20 mg/L (LCK 350)	Germany	±5–10%
UF Unit			Germany	±5–10%
COD	Photometric Method	Hach Lange Test Kit Method COD 100–2000 mg/L (LCK 514)	Germany	±5–10%
NH_4-N	Photometric Method	Hach Lange Test Kit Method NH_4-N 1–12 mg/L (LCK 305), 2–47 mg/L (LCK 303)	Germany	±5–10%
TN	Photometric Method	Hach Lange Test Kit Method	Germany	±5–10%
PO_4-P	Photometric Method	Hach Lange Test Kit Method	Germany	±5–10%
DO	Photometric Method	Hach Lange HQ40d-Hach LDO-Lange SC 1000 differential online	Germany	±5–10%
Nitrate (NO_3-N)	Photometric Method	Hach Lange Test Kit Method NO_3-N 0.23–13.5 mg/L (LCK 339)	Germany	±5–10%
Nitrite (NO_2-N)	Photometric Method	Hach Lange Test Kit Method NO_2-N 0.6–6 mg/L (LCK 514)	Germany	±5–10%
NF Unit			Germany	±5–10%
COD	Photometric Method	Hach Lange COD 15–150 mg/L (LCK 314)	Germany	±5–10%
NH_4^+-N	Photometric Method	Hach Lange NH_4-N 1–12 mg/L (LCK 305), 0.015–2 mg/L (LCK 304)	Germany	±5–10%
TN	Photometric Method	Hach Lange Test Kit Method	Germany	±5–10%
PO_4-P	Photometric Method	Hach Lange Test Kit Method	Germany	±5–10%
pH		Online pH Meter (Endress Hauser)	Switzerland	±0.01

2.4. Treatment System Overview

Membrane Bioreactor, Nanofiltration and Ultrafiltration System

The MBR system integrates biological treatment with physical filtration. In this process, organic matter is degraded through microbial activity, and the resulting treated liquid is directed to the NF unit. The operating conditions of the MBR are optimized based on key parameters such as the MLSS, DO levels, and temperature [25–28]. NF is an effective advanced treatment method for removing dissolved solids and trace pollutants. After biological treatment in the MBR, the effluent is directed to the NF unit, where residual minerals, organics, and harmful substances are removed. The efficiency of NF membranes depends on factors such as the operating pressure, flow rate, and recovery ratio [15,29].

The MBR system incorporates UF membranes for solid–liquid separation, preventing biomass and suspended solids (SS) from passing into the NF stage. Operating in cross-flow mode, the UF unit minimizes membrane fouling and ensures consistent filtrate quality. System performance is optimized through the real-time monitoring of DO, MLSS, and

temperature. The schematic diagram of the treatment process is presented in Figure 1, and the bioreactor design parameters are listed in Table 4.

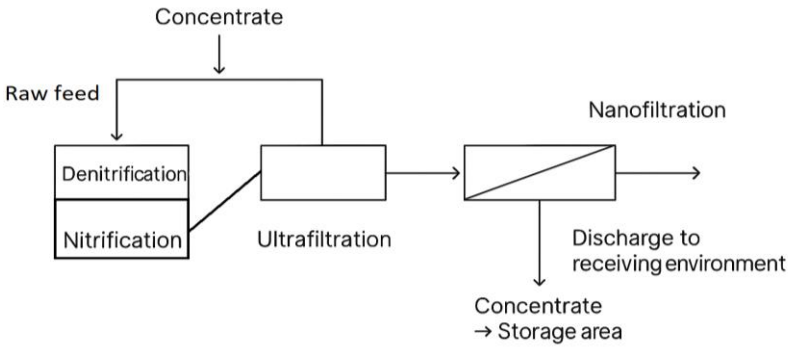


Figure 1. Treatment plant process flow chart.

Table 4. Bioreactor design criteria.

Parameter	Unit	Value
Design capacity	m^3/day	1200 ± 50
Reactor volume	m^3	20,000 ± 1000
MLVSS	mg/L	8000–15,000 ± 500
Biomass yield coefficient	kg solids/kg COD	0.25 ± 0.02
Sludge loading (F/M)	kg COD/kg TSS	0.08–0.15 ± 0.01
Sludge age	day	>20 ± 2
Hydraulic Retention Time (HRT)	day	16.7 ± 0.5

The bioreactor consists of two main compartments: an anoxic and an aerobic zone (Figure 2). Leachate first enters the anoxic section, where denitrification occurs. In this zone, the nitrate and nitrite generated via nitrification are converted into nitrogen gas with the aid of BOD_5. In cases where the incoming leachate has an insufficient carbon content, methanol is added to maintain effective denitrification. The pH in this section is maintained between 8.0 and 8.4.



Figure 2. Bioreactor view.

In the aerobic zone, COD is oxidized to CO_2 and biomass, while organic nitrogen is first converted to ammonium and, under sufficient oxygen conditions, further oxidized to nitrate and nitrite. Three types of aeration equipment are employed: surface aerators, blowers, and jet aerators. The excess sludge generated during biological treatment is dewatered using a thickener and a centrifugal decanter before disposal.

Following biological treatment, the leachate enters the membrane system, which includes two stages: ultrafiltration and nanofiltration. Prior to the UF unit, a coarse pre-filtration is conducted using 2 mm steel mesh filters installed between the feed and

circulation pumps. These filters protect the system from damage caused by larger particles and are cleaned periodically (Figure 3).



Figure 3. Coarse screen.

The UF unit (Figure 4) is the first membrane step and is responsible for separating sludge from the biologically treated water. Tubular UF membranes made of polyvinylidene fluoride (PVDF) are installed externally to the bioreactor in a cross-flow configuration, which is common in industrial-scale MBRs. This setup supports high flow rates and reduces fouling through turbulence generated at a flow velocity of 4 m/s (Table 5). Circulation pumps maintain the necessary pressure across the modules.



Figure 4. Ultrafiltration membrane unit.

Table 5. Ultrafiltration unit design criteria.

Parameter	Unit	Value
Design Capacity, max	m^3/day	1200
Unit	piece	4
Module per Unit	piece	6
Total Module	piece	24
Membrane Area	m^2	-
Membrane Area per Unit	m^2	162
Total Membrane Area	m^2	648
Operating Flux	lmh	77
Average Permeate Flow Rate	m^3/hour	50
UF Concentration Factor	-	1.2
Flow Velocity	m/s	4

Each UF membrane module has a pore size of 20 nanometers and a surface area of approximately 27 m^2. The system is designed as a skid-mounted unit containing six modules per skid. On average, each module provides a permeate flow rate of 2 m^3/h, with pressure losses ranging from 0.9 to 1.1 bar. External membrane modules were preferred

over immersed types due to the more aggressive nature of landfill leachate compared to domestic wastewater.

Membrane fouling is one of the most common operational challenges. Routine backwashing is applied to mitigate fouling during normal operation. If this is insufficient, chemical cleaning (CIP—Clean-in-Place) is initiated, typically every 4–6 weeks, depending on the membrane performance and transmembrane pressure conditions. Acidic CIP involves heating water to 38 °C and adjusting the pH to 1.8 using 37% HCl, circulating the solution through the membranes at 1.7 bar for 2 h. In the case of persistent organic fouling, alkaline cleaning with NaOH or Ultrasil at pH 11 is performed. This solution is circulated for 1 h, soaked for an additional hour, and repeated to complete a 4 h cycle. If chemical cleaning proves ineffective, physical cleaning is carried out by manually flushing the disconnected modules with clean water at 4–6 bar using a metal container. This method is used with caution to prevent membrane damage.

The biologically treated, solids-free effluent from the UF unit is further processed in the NF stage, which utilizes spiral wound membranes (Figure 5). In this step, non-biodegradable BOD, heavy metals, monovalent and divalent ions, as well as odor and color, are removed. The system operates in cross-flow mode to minimize fouling. The NF system comprises two units, each containing 14 pressure vessels. Each vessel holds six spiral wound membrane modules connected in series. These membranes are designed to produce a high recovery rate (90%) and a low concentrate volume (10%). The concentrated stream is recirculated back to a holding tank in a controlled manner via dedicated channels. Table 6 outlines the design specifications of the NF unit.



Figure 5. Nanofiltration membrane unit.

Table 6. Nanofiltration unit design criteria.

Parameter	Unit	Value
Capacity	m^3/day	1200
Unit	piece	2
Pressure Vessel per Unit	-	10
Module per Pressure Vessel	-	6
Total Module	-	120
Membrane Area per Module	m^2	25.3
Membrane Area per Unit	m^2	1518
Total Membrane Area	m^2	3036
Operating Flux	Lmh	16.5
Average Feed Flow Rate	m^3/h	50
Recovery Rate	%	≥90
Recirculation Flow Rate per Unit	m^3/h	30

2.5. Artificial Neural Network Modeling

AI refers to the development of computer systems capable of performing tasks that typically require human intelligence, such as decision-making, pattern recognition, and problem-solving. By analyzing environmental data, AI systems can learn from past experiences and optimize future decisions accordingly. The application of AI is widespread in fields such as image and speech recognition, natural language processing, robotics, and environmental engineering, including wastewater treatment [30]. In this study, ANN modeling was employed to predict key effluent quality parameters, including the COD and NH_4-N concentrations, based on the influent characteristics and operational conditions.

2.5.1. Structure and Functioning of ANN

ANN is based on a collection of connected units or nodes called artificial neurons, which loosely model the neurons in a biological brain. Each neuron processes input signals by applying a weight to them and passes the result through a non-linear activation function. Typically, neurons are grouped into layers: an input layer receives data from the external environment, hidden layers transform these data through weighted computations, and an output layer delivers the final result (Figure 6). Each neuron in a layer is connected to all neurons in the subsequent layer, forming a fully connected feedforward network. This architecture enables the network to learn complex nonlinear patterns from data. Such models have been widely used in environmental systems modeling, including the prediction of pollutant removal efficiencies in wastewater treatment processes [31].

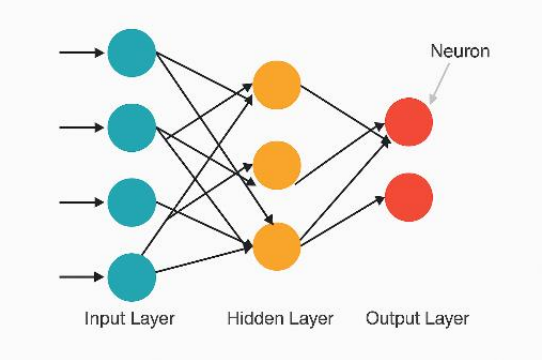


Figure 6. Schematic architecture of a feedforward ANN model.

2.5.2. Model Development Process

The ANN model in this study was developed using operational and water quality data collected from the landfill leachate treatment plant. Five input variables were selected:

- Influent COD concentration (mg/L)
- NH_4-N concentration (mg/L)
- Suspended solids (SS, mg/L)
- Aeration basin temperature (°C)
- MLSS concentration (g/L)

The output layer consisted of two parameters:

- COD concentration after ultrafiltration (mg/L)
- NH_4-N concentration after ultrafiltration (mg/L)

A total of 243 complete datasets were used in the modeling process. Of these, 170 records were used for training, 61 for testing, and 12 for validation (Figure 7). Data preprocessing included min–max normalization, the elimination of incomplete records, and outlier detection through time-series visual inspection and reference to plant operation logs. These steps were essential to ensure model robustness, reproducibility, and accuracy. The

range (min–max) of the input and output parameters used in the ANN model is provided in Table 7.

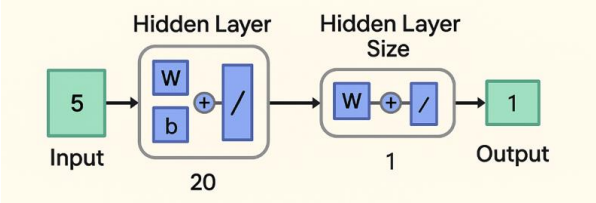


Figure 7. Data distribution for training, testing, and validation.

Table 7. Minimum and maximum values of the study parameters.

Parameter	Unit	Max	Min	Avg	Std. Dev.
COD_{inlet}	(mg/L)	33,925	14,055	23,080	4145
NH_4-N_{inlet}	(mg/L)	3000	1525	2250	300
SS_{inlet}	(mg/L)	1870	350	731	202
Temperature	(°C)	29.8	9	21.3	7.9
$MLSS_{MBR}$	(mg/L)	18,500	12,010	15,040	1346
NH_4-$N_{MBR\ outlet}$	(mg/L)	234	0.4	45	56.8
$COD_{MBR\ outlet}$	(mg/L)	2345	815	1365	265.5

2.5.3. Network Structure and Training Method

To determine the optimal ANN architecture, 20 different network configurations were tested. Each configuration varied in the number of hidden layers and processing elements. A feedforward back-propagation algorithm was used for model training, and model performance was evaluated based on the mean squared error (MSE) between the observed and predicted values [32,33].

The best-performing model architecture included 20 hidden processing elements. This configuration yielded the highest correlation between the predicted and observed results (Figure 8). During training, the network iteratively adjusted the connection weights to minimize the prediction error and enhance generalization on unseen data.

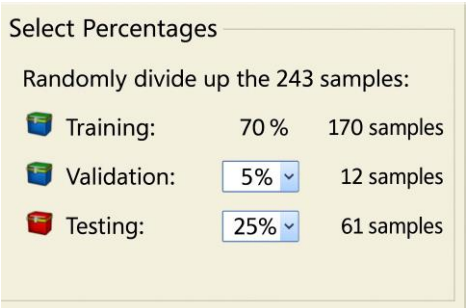


Figure 8. Feedforward back-propagation model structure.

2.5.4. Model Validation Metrics

The model's performance was quantified using the following metrics. First, the root mean squared error (RMSE) was calculated using Equation (2):

$$RMSE = \sqrt{\frac{1}{n}\sum_{i=1}^{n}(y_i - \hat{y}_i)^2} \quad (2)$$

where y_i is the observed value, $\hat{y}_i$ is the model prediction, and n is the total number of samples. Second, the mean absolute error (*MAE*) was computed according to Equation (3):

$$MAE = \frac{1}{n}\sum_{i=1}^{n}|y_i - \hat{y}_i| \quad (3)$$

which represents the average magnitude of prediction errors regardless of direction. To assess the statistical uncertainty of these metrics, 95% confidence intervals (CI) were estimated via a nonparametric bootstrap procedure: the original dataset was resampled with replacement B = 1000 times, and *RMSE* and *MAE* were recalculated for each bootstrap replicate. The lower and upper bounds of the 95% CI correspond to the 2.5th and 97.5th percentiles of the resulting bootstrap distributions for each metric.

2.6. Assumptions and Limitations

Several assumptions were made during the design, operation, and modeling phases of this study:

Steady-State Operation: It was assumed that the biological treatment units operated under pseudo-steady-state conditions during each sampling period, despite known seasonal variations.

Uniform Influent Characteristics: The influent characteristics were considered representative and sufficiently stable to generalize the system's removal efficiencies over time.

Constant Membrane Performance: The membrane fouling and cleaning cycles were considered consistent, and the effective membrane surface area was assumed not to change significantly over time.

Negligible Measurement Errors: Analytical measurements were assumed to be within the acceptable error margins provided by the manufacturers (±5–10%), and instrument calibration was regularly performed.

ANN Model Assumptions:

Input data were assumed to be free from multicollinearity and adequately normalized.

The training and testing datasets were assumed to represent the overall population distribution.

Outlier effects were minimized via visual inspection and operational logging, assuming no significant unaccounted disturbances.

These assumptions allowed for simplified modeling and interpretation, but may also limit the extrapolation of results to significantly different operational contexts.

3. Results

3.1. Wastewater Characterization

According to Table 8, the COD levels of the leachate are very high, with an average above 20,000 mg/L, indicating a very high organic pollutant load. This implies that the wastewater contains substantial amounts of biodegradable and non-biodegradable substances. The wide range and high standard deviation show considerable variability, possibly due to fluctuating industrial discharges or influent compositions [34,35]. The concentration of NH_4-N is quite elevated, reflecting the presence of high nitrogenous waste, likely from domestic or industrial effluents. The relatively low standard deviation suggests moderate variability across the samples [34,36]. High PO_4-P levels are typically linked to detergents or agricultural runoff. The moderate standard deviation indicates consistent high levels, which could pose a risk of eutrophication if the wastewater is discharged into natural water bodies without proper treatment. TP is also considerably high, which reinforces concerns regarding the risk of eutrophication. The lower variability suggests a stable but consistently high TP input [37,38]. The SS levels show moderate

to high values. This can negatively affect aquatic habitats by increasing turbidity and reducing light penetration. The moderate standard deviation reflects a somewhat stable particle load [39,40]. The temperature range suggests the wastewater is affected by seasonal or operational changes. A wide standard deviation confirms this variability, which can influence microbial activity and biological treatment efficiency [41,42]. The pH values are within a slightly alkaline range, suitable for most biological treatment processes. The low standard deviation indicates a very stable pH condition, which is favorable for maintaining microbial populations [43].

Table 8. Leachate measurements.

Parameter	Unit	Maximum	Minimum	Average	Standard Deviation	CV (%)
COD	mg/L	33,925	9555	20,795	4980	23.9
NH_4-N	mg/L	3300	1237	2195	315	14.3
PO_4-P	mg/L	24.5	1.7	11.3	3.3	29.2
TP	mg/L	26.3	9.4	16.8	2.98	17.7
TSS	mg/L	1870	350	720	190	26.4
Temperature	°C	29.8	6.9	18.4	5.74	31.2
pH	-	8.7	7.3	8	0.18	2.3

This dataset represents a high-strength wastewater with substantial organic matter (high COD), nitrogen, and phosphorus concentrations. Such compositions can significantly challenge treatment systems and pose environmental risks if not properly managed. Regular monitoring and advanced treatment technologies may be necessary to meet discharge standards.

3.2. Performance of the Biological Treatment Unit

3.2.1. Temperature Effect

Bioreactor temperatures ranged from 8.9 °C to 29.1 °C. Optimal COD and ammonium removal efficiencies were observed above 15 °C, where microbial activity was more robust. Seasonal temperature fluctuations aligned with the influent and reactor measurements, confirming their influence on biological performance (Table 9).

Table 9. Temperature variation in the bioreactor.

Temperature, °C	Max	Min	Avg	Std. Dev.
Aeration Tank	29.1	8.9	19.8	5.28
Anoxic Tank	27.5	9.7	19.4	4.67

Figure 9 shows the daily temperature changes from the beginning of 2009 until the spring of 2010 for three different environments: Influent, Aerobic and Anoxic temperatures. In general, all three temperature types show similar trends, with low temperatures in winter and high temperatures in summer. In summer, temperatures approach 30 °C, while in winter they drop as low as 8 °C. The influent temperature is often slightly below the other two temperature types, indicating that treatment processes may be slightly more stable and warmer in the indoor environment. Aerobic and anoxic temperatures are quite close to each other and are usually higher. Especially in summer, the difference between the temperatures is minimal, indicating that the environmental heat effect is evident in all environments. Overall, there is a clear summer–winter oscillation in all temperature types, consistent with seasonal cycles.

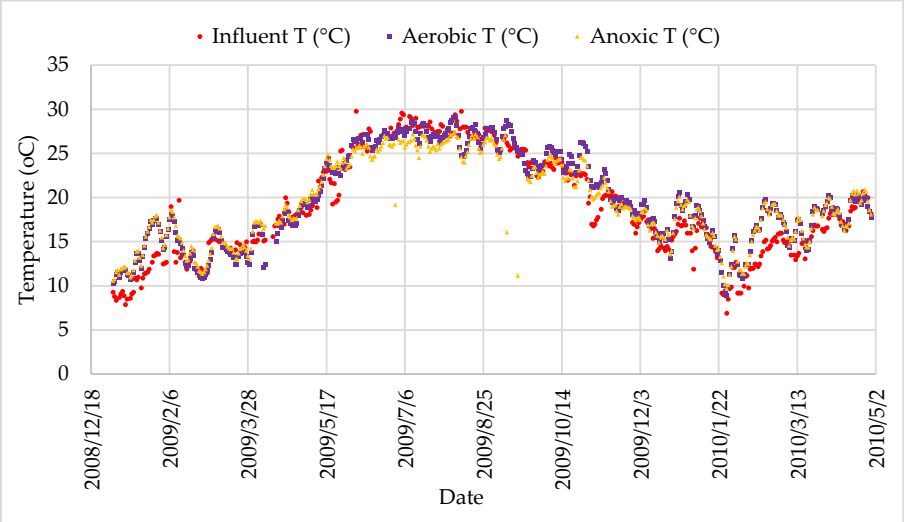


Figure 9. Daily temperature changes.

3.2.2. Biomass Concentration

The average MLSS was approximately 13,900 mg/L in the aeration tank, enabling efficient organic matter degradation and nitrification processes (Table 10).

Table 10. Concentration values of MLSS in aerobic and anoxic tanks.

Tank	Max (mg/L)	Min (mg/L)	Mean (mg/L)	Std. Dev. (mg/L)
Aeration Tank	18,500	7200	13,900	2460
Anoxic Tank	18,100	7000	13,700	2250

Figure 10 illustrates the time-dependent variation in the influent SS and MLSS concentrations between early 2009 and mid-2010. The influent SS values are generally low, fluctuating around 1–2 g/L, although occasional sudden spikes are observed. In contrast, the MLSS concentrations in both the anoxic and aerobic zones remain relatively stable within the range of 10–17.5 g/L. A noticeable upward trend in MLSS levels is evident after May 2009, despite some short-term declines, such as the drop in February 2010. These fluctuations likely reflect operational changes, system malfunctions, or possible measurement inconsistencies.

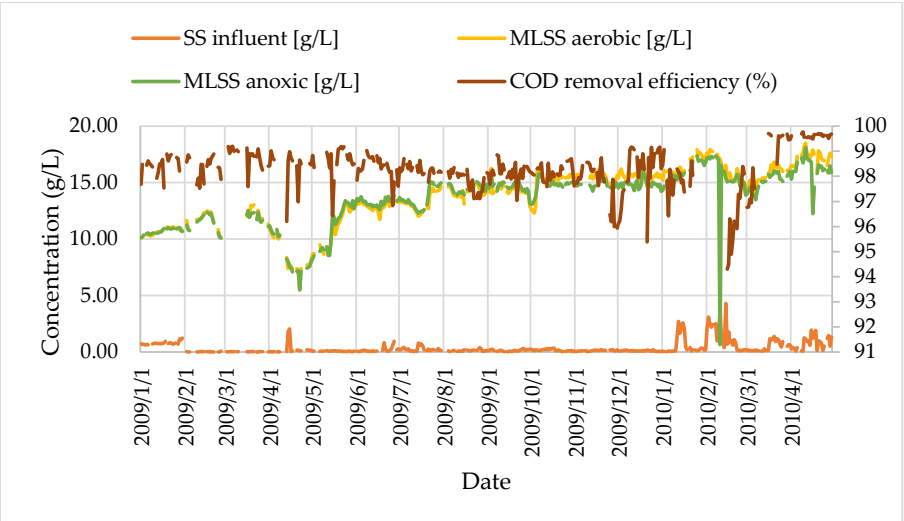


Figure 10. The time-dependent change in SS influent and MLSS concentrations.

The concurrent evaluation of influent SS and MLSS is crucial for tracking the performance of the biological treatment process. While influent SS represents the incoming pollutant load, MLSS concentrations are indicative of biomass activity and overall system efficiency. Sudden increases in influent SS can lead to temporary stress on the system, potentially reducing short-term COD removal efficiency [44]. However, these impacts appear to be limited in the long run [45].

Elevated MLSS in the anoxic zone supports enhanced denitrification, indirectly contributing to COD reduction, whereas higher MLSS in the aerobic zone directly improves COD removal through more effective organic matter oxidation [45]. Furthermore, Figure 10 demonstrates that MLSS trends align with seasonal temperature changes, emphasizing the sensitivity of microbial activity to environmental conditions and underscoring the operational resilience of the treatment system.

3.2.3. Dissolved Oxygen

DO concentrations in the aeration tank ranged from 0.09 to 9.17 mg/L, with higher values positively impacting COD removal. In contrast, the anoxic tank maintained DO levels between 0–1.3 mg/L, appropriate for denitrification (Table 11).

Table 11. Variation in dissolved oxygen concentration in the bioreactor.

Dissolved Oxygen Concentration (mg/L)	Max	Min	Average	Std. Deviation
Anoxic Tank	1.30	0.00	0.30	0.55
Aeration Tank	9.17	0.09	3.66	1.73

Figure 11 presents dissolved oxygen (DO) measurements recorded between January 2009 and May 2010, separately for the aerobic and anoxic zones of the treatment system.

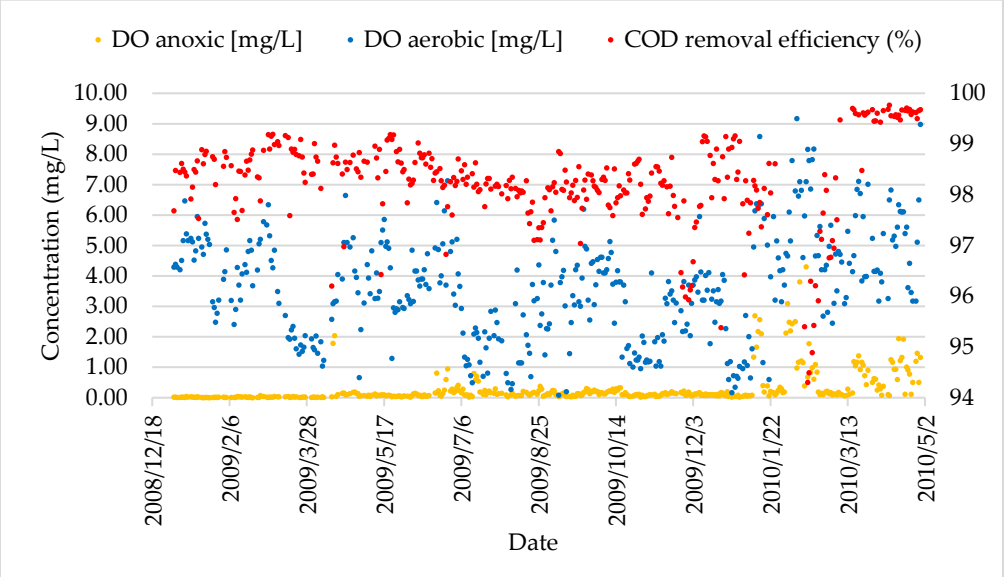


Figure 11. Relationship between DO values in anoxic and aeration tank with COD removal efficiency.

In the aerobic environment, the DO concentrations generally ranged between 2 and 9 mg/L, indicating that the system operated under the oxygen-rich conditions suitable for biological treatment. Although the data exhibit some variability, the values remained within a stable and acceptable range throughout the monitoring period.

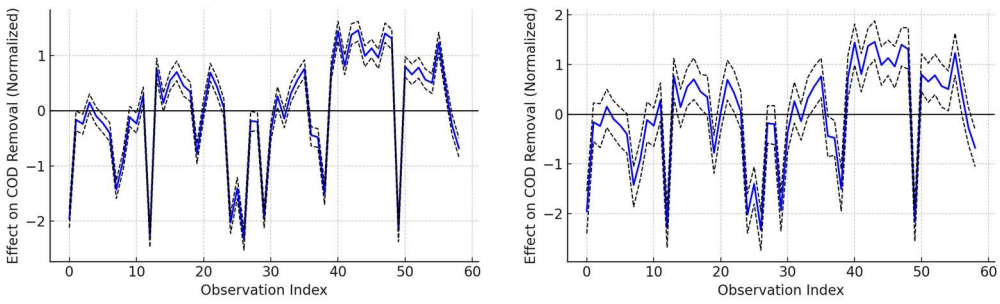
In contrast, the anoxic DO concentrations ranged from 0 to 1.3 mg/L, with most values clustering around 0.2–0.4 mg/L, suggesting that anoxic conditions were effectively

maintained—an essential requirement for denitrification. Although short-term increases above 0.5 mg/L were occasionally observed, these fluctuations did not appear to adversely impact the system's overall performance.

The data demonstrate that the treatment system successfully maintained both aerobic and anoxic conditions over time. Furthermore, a positive correlation was observed between the aerobic DO levels and COD removal efficiency, with higher COD removal rates corresponding to adequate oxygen availability. Conversely, the relationship between anoxic DO and COD removal appeared weaker and more indirect. Sudden fluctuations in DO, particularly in the anoxic zone, may have adversely affected COD removal to a limited extent.

Overall, Figure 11 confirms that appropriate DO levels were consistently achieved and maintained in the biological treatment process. Sufficient oxygen was supplied in the aerobic tank to support efficient nitrification, while low DO levels in the anoxic tank provided favorable conditions for denitrification.

The blue line in Figure 12a shows the 15-day effect of a sudden increase of 1 unit in the aerobic oxygen level on COD removal efficiency. A slight increase started in the first 3 days. From day 5, a strong positive effect is observed. The effect reached its maximum around day 8 (~0.17 standard deviation units). Then, the effect decreased and stabilized, i.e., the system adapted to the new oxygen levels. This analysis shows that increasing dissolved oxygen in the aerobic environment significantly improves the COD yield. Figure 12b shows the 15-day effect of a sudden increase of 1 unit in the anoxic DO level on the COD removal efficiency. An unstable and weak response is observed in the first 3 days. Around day 6–7, there is a slight positive effect for a short time, but this is not permanent. From day 9 onwards, the effect is negative, but weak. Throughout the entire analysis, the effect appears to be within the confidence interval and not statistically significant.



(**a**) Aerobic impulse-response analysis. (**b**) Anoxic impulse-response analysis.

Figure 12. Effect–response analysis between dissolved oxygen and COD removal efficiency under aerobic and anoxic conditions.

Effect–response analyses show that increases in DO levels in an anoxic environment do not have a significant and consistent effect on COD efficiency. The efficiency of the system depends more on the aerobic oxygen levels.

3.2.4. pH Stability

The pH values in the aerobic and anoxic reactors remained between 5.9 and 9.0, supporting microbial stability (Table 12). A temporary drop observed in early 2010 may relate to operational or environmental disturbances.

Table 12. Variation in pH in bioreactors.

Reactor Type	Max pH	Min pH	Average pH	Std. Deviation
Aeration Tank	9.0	5.9	8.2	0.36
Anoxic Tank	8.8	6.0	8.0	0.35

Figure 13 shows how the pH values in the three different stages of the wastewater treatment process (Influent, Aerobic, and Anoxic) changed over time from early 2009 to mid-2010. In general, the pH values fluctuate between 7.5 and 8.5, with Influent values generally slightly lower than the other two stages. Especially in February-March 2010, a significant pH drop is observed in all stages, possibly due to an unusual situation such as a system failure, an environmental change, or a chemical intervention. The pH values in the Anoxic and Aerobic stages are very close to each other, suggesting consistent control of the chemical balance in the treatment process. Considering the general trends, it seems that pH control was successfully maintained throughout most of the system.

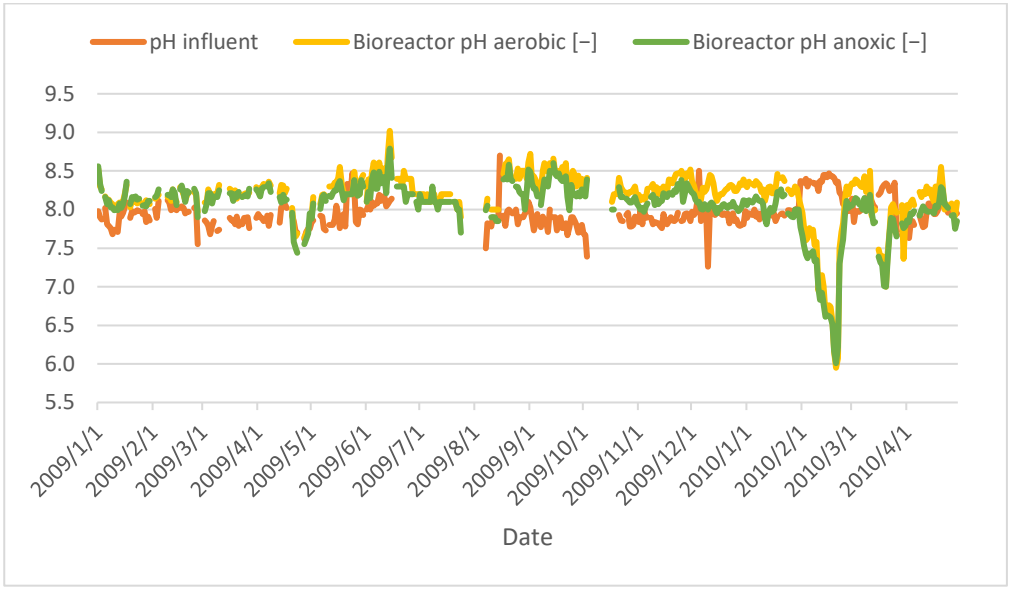


Figure 13. Variation in pH values of MBR under aerobic and anoxic conditions.

3.3. Nutrient Removal Performance

3.3.1. Nitrogen Removal

MBR demonstrated NH_4-N removal rates exceeding 98%. TN removal was highly efficient (90–100%) in both the MBR and overall system, while NF contributed variably due to potential operational inconsistencies.

Figure 14 shows the TN removal efficiency of the MBR, NF and plant, as well as the NH_4-N removal efficiency of the MBR system in percentages between 1 January 2009 and 1 April 2010. The MBR TN removal efficiency and TN removal efficiency showed a very high and stable performance, generally in the range of 90–100%. This shows that the MBR system provides the most critical contribution both on its own and for the plant as a whole. The MBR NH_4-N removal efficiency was also generally high (around 90%), with short-term declines in late 2009 and early 2010. These decreases can be explained by factors affecting biological nitrogen removal, such as temperature, oxygen deficiency, or a decrease in microbial activity. The NF TN removal efficiency, on the other hand, fluctuated significantly, ranging from 0 to 80%, with a significant decline in performance, especially from the end of 2009. These data indicate that there may be operational problems in the NF system, while the MBR system is quite successful in overall TN and NH_4-N removal.

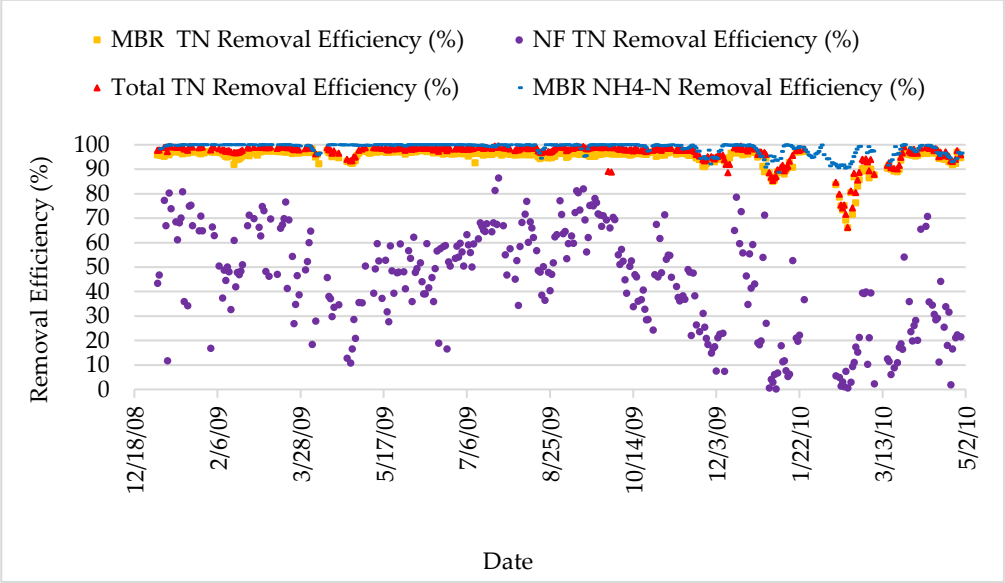


Figure 14. Total nitrogen and ammonium nitrogen removal efficiency.

3.3.2. Nitrogen Removal Regression Analysis

As a result of the regression analysis between the MBR TN removal efficiency and MBR COD removal efficiency, the regression coefficient was 0.842 and the R^2 value was 0.211. A 1% increase in the MBR TN removal efficiency corresponds to an increase of approximately 0.84% in the MBR COD removal efficiency. However, since the R^2 value is only 0.211, this relationship indicates a weak linear relationship. In other words, TN removal has a limited effect in explaining COD removal and other variables should be considered to be effective in removal.

According to the regression analysis between the NF TN removal efficiency and NF COD removal efficiency, the R^2 value obtained was 0.1346. This low R^2 value indicates that the power of NF COD values to explain TN removal efficiency is weak. That is, NF COD removal alone is not a strong determinant of NF TN removal.

According to the results of the regression analysis, the regression coefficient is 2.81 and R^2 value is 0.27. According to these results, there is a positive but weak linear relationship between the total COD removal and TN removal efficiency. That is, approximately 27% of the change in total COD explains the change in the TN removal efficiency.

3.4. Phosphorus Removal Performance

3.4.1. Phosphorus Removal

TP removal was primarily achieved by NF, reaching consistent efficiencies above 95%. MBR and UF showed an increasing removal efficiency over time (up to ~90%), indicating synergy between biological and membrane processes. Table 13 presents the PO_4-P concentrations in the MBR effluent, whereas Table 14 shows the TP concentrations in the NF effluent.

Table 13. PO_4-P variation in the bioreactor.

Concentration (PO_4-P), mg/L	Max	Min	Avg	Std. Dev.
MBR Effluent (UF)	15	0.06	1.43	1.99

Table 14. TP variation in the bioreactor.

Concentration (TP), mg/L	Max	Min	Avg	Std. Dev.
NF Effluent	11.8	0.12	0.69	1.16

Figure 15 shows the TP removal efficiencies of the MBR, UF and NF systems between 1 January 2009 and 1 July 2009. The TP removal efficiencies (%) of the MBR and UF systems overlap to a great extent and the efficiency, which started around 20% at the beginning, increased over time and reached 80–95%. This indicates that the UF system is most likely processing the MBR effluent and therefore exhibits similar efficiency profiles. However, in early April 2009, both systems showed a sudden drop (up to 50%), which could be the effect of a possible breakdown, maintenance or a temporary disruption in the process. The TP removal efficiency of the NF system was more constant and generally around 95%, showing a high and stable performance except for small fluctuations. In general, this graph shows that the efficiency of the systems increases over time, but there are common performance decreases in some periods and the NF system gives the most stable results in phosphorus removal.

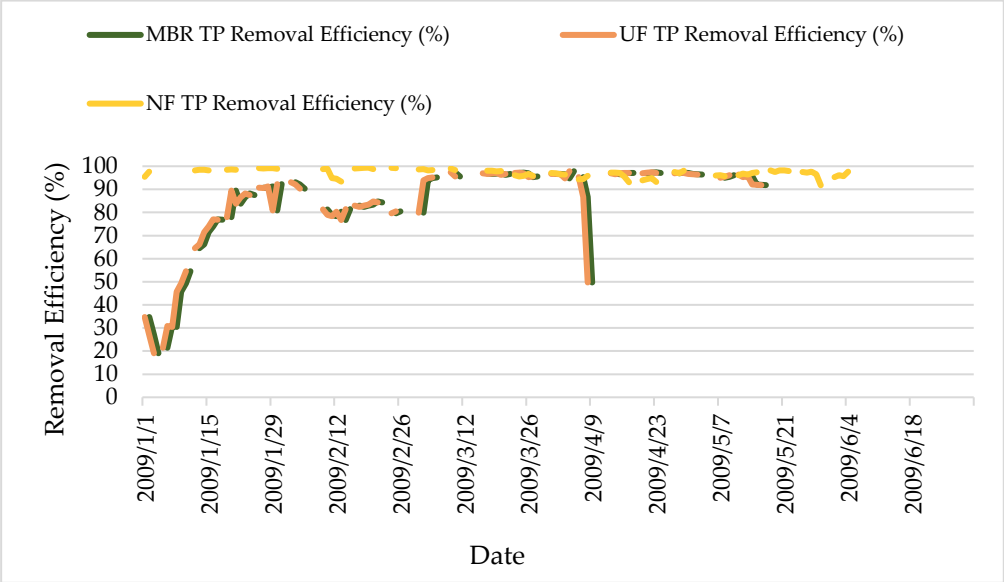


Figure 15. TP removal efficiency.

Although the TP removal performance of the NF unit was generally high and stable (average > 95%), occasional fluctuations were observed in the effluent TP concentrations. This variability can be attributed to several operational and physicochemical factors. First, membrane fouling—especially organic or biofouling—can temporarily reduce the TP rejection efficiency by altering the surface characteristics or permeability of the membranes. Second, pressure fluctuations and changes in the recovery ratio may affect the selective rejection of phosphates. In periods of high flux or suboptimal cross-flow velocity, the breakthrough of low-molecular-weight phosphorus species may occur. Third, the incomplete upstream removal of phosphorus in the MBR unit can increase the phosphorus load on the NF system, thereby affecting its performance. Additionally, fluctuations in the influent pH may influence the ionic state of phosphate species, which can alter membrane rejection behavior. These factors together explain the observed short-term variability in TP concentrations in the NF effluent, despite the generally high average removal rates.

3.4.2. Phosphorus Removal Regression Analysis

According to the regression analysis between the MBR TP and MBR COD removal efficiency, the R^2 value is 0.48. This indicates that TP removal has an explanatory effect of 48% on COD. In the regression analysis between the NF COD and NF TP removal efficiency, the R^2 was 0.093. The explanatory power of the model is low; it explains only 9.3% of the variable. The *p*-value is 0.018, which is statistically significant at a 5% significance level.

3.5. COD Removal Performance

MBR achieved stable and high COD removal (avg. 93.5%), while the NF performance fluctuated significantly (avg. 72.3%) (Table 15). The total system COD removal consistently exceeded 98%, confirming the dominance of MBR in organic pollutant removal and the polishing role of NF.

Table 15. Treatment efficiency based on parameters.

Parameter	Treatment Type	Max	Min	Avg	Std. Dev.
COD (%)	MBR Removal Efficiency	96.92	86.31	93.52	1.97
	NF Removal Efficiency	96.40	10.40	72.31	14.62
	Total Removal Efficiency	99.77	94.30	98.29	0.86
NH_4-N (%)	MBR Removal Efficiency	99.98	88.67	98.60	2.31
TP (%)	MBR Removal Efficiency	97.84	19.06	84.78	18.63
	Total Removal Efficiency	99.14	90.71	97.44	1.92

In Figure 16, the COD removal efficiencies of MBR, NF and the total system are compared between 2 January 2009 and 2 April 2010. The MBR system shows that COD removal is a very successful and reliable process, with a constant and high performance above 90%.

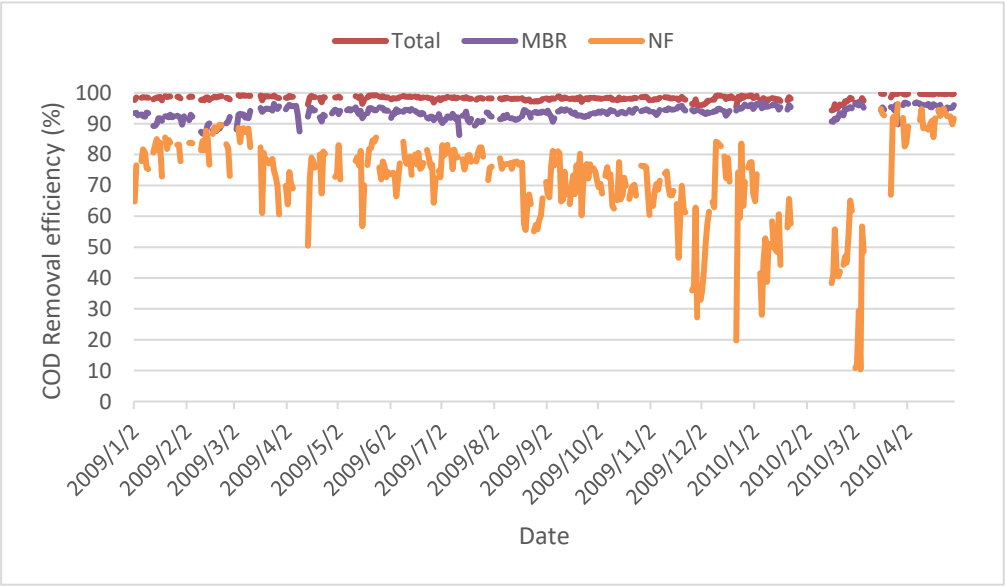


Figure 16. COD removal efficiencies of MBR, NF and total system.

The total system efficiency is also in parallel with MBR, suggesting that MBR plays a dominant role in the system performance. On the other hand, the efficiency of the NF system fluctuates significantly over time, approaching 90% in some periods and dropping to 0% in others. This instability in the NF system could be caused by membrane fouling, changes in the operating conditions or problems in process control.

To compare the performance of the MBR and NF treatment stages, both paired *t*-test and one-way ANOVA were conducted (Table 16). The paired *t*-test revealed a statistically significant difference in the COD removal efficiencies between the two systems ($p < 0.001$), indicating the superior performance of the MBR. This was further supported by the ANOVA results ($p < 0.001$), which confirmed a significant overall difference between the treatment stages. On average, the MBR achieved a COD removal efficiency of 93.6%, notably higher than the 72.3% achieved by the NF unit. This performance gap is both statistically and practically significant.

Table 16. To compare the performance of MBR and NF treatment stages.

Test Type	Test Statistic	*p*-Value	Comment
Paired *t*-test	26.18	2.85×10^{-84}	Significant difference between MBR and NF
One-way ANOVA	726.51	3.89×10^{-110}	In general, there is a difference between the groups.

The provided heatmap shows the correlations between the removal efficiencies of different pollutants (COD, TN, TP) in wastewater treatment processes involving MBR and NF (Figure 17). There is a very high positive correlation between the removal of COD and TP across all treatment methods. This indicates that the processes effective at removing COD are also effective at removing TP. Total COD removal is highly correlated (0.98–1.00) with TP removal (MBR, NF, and Total TP removal). This suggests a similar operational efficiency for these pollutants. MBR TP removal and NF TP removal also show high positive correlations (around 0.95–1.00), indicating a consistent TP removal performance between the two membrane types.

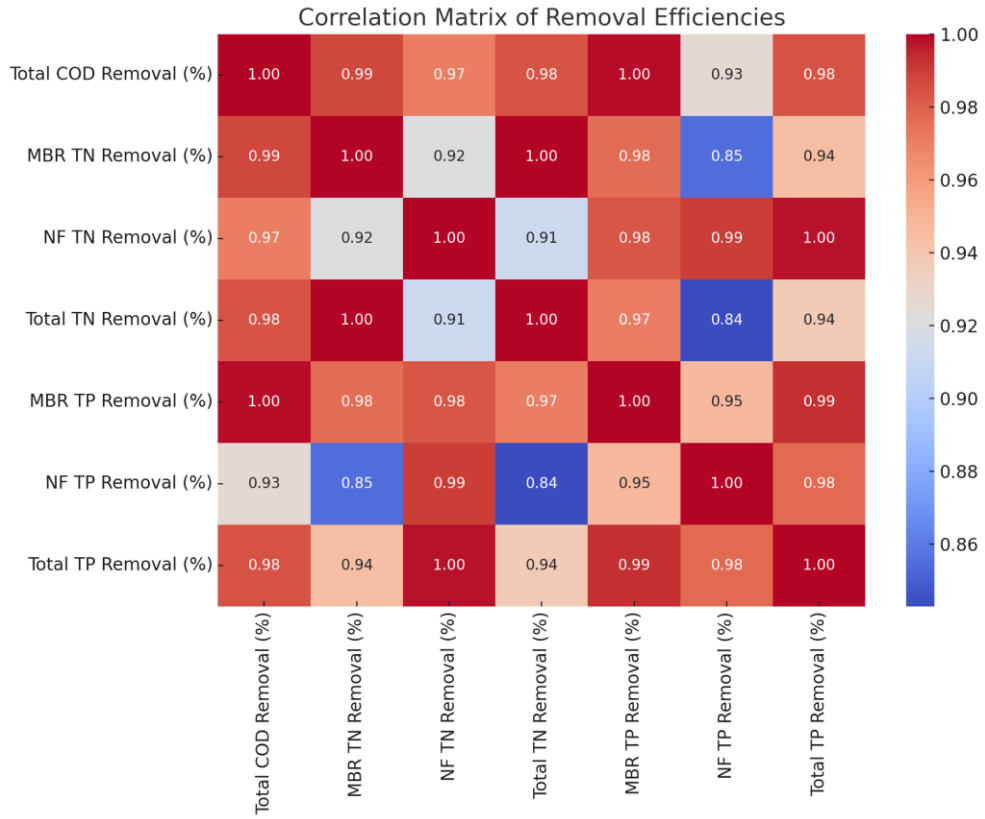


Figure 17. The correlation matrix between the total COD, TN and TP removal efficiencies.

The correlations between TN removal and other parameters are moderate to high (around 0.91–0.99). This suggests that TN removal tends to follow similar trends to COD and TP removal, though slightly weaker.

The lowest correlations (0.84–0.92) occur between NF TN removal and other parameters, especially with MBR TN removal (0.85) and NF TP removal (0.84). These relatively lower values imply that NF TN removal has a slightly different pattern or efficiency compared to TP removal processes or MBR treatment.

The high correlation values indicate that wastewater treatment processes (particularly MBR and NF) have closely related efficiencies in removing COD and TP, while TN removal efficiencies vary slightly more distinctly. This matrix helps illustrate that optimizing COD or TP removal is likely to simultaneously enhance the removal efficiency of other pollutants, though TN removal might need specific attention due to slightly different removal behaviors.

3.6. Confidence Interval and Comparative Analysis of MBR and NF Performance

In Figure 18, the removal efficiencies of MBR and NF are statistically evaluated. In the figure, the columns show the average removal percentages and the error bars show the 95% confidence intervals. As can be seen in Figure 18, the MBR system shows a high and stable performance in terms of both COD and NH_4-N. The NF system operates with lower mean and larger uncertainty (high standard deviation). To address uncertainty in the performance data, 95% confidence intervals were calculated and added to the COD and ammonium removal results. Error bars were included in the related figures to visually represent the statistical variation in treatment performance.

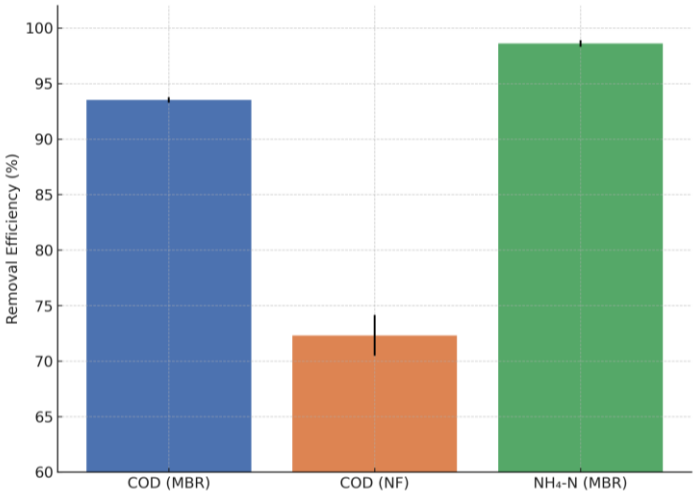


Figure 18. Statistical analyses of the removal efficiencies of MBR and NF.

3.7. Results Obtained with ANN and Principal Component Analysis (PCA)

This section presents the results obtained from the ANN modeling and Principal Component Analysis (PCA) applied to predict and analyze the performance of the MBR system in removing COD and ammonium from landfill leachate.

3.7.1. ANN Modeling Results for COD and Ammonium

An ANN model was developed to estimate the effluent concentrations of COD and NH_4-N from the MBR unit based on five input parameters: $COD_{influent}$, $NH_4\text{-}N_{influent}$, $TSS_{influent}$, temperature, and MLSS. The model performance was evaluated using the coefficient of determination (R^2).

Table 17 summarizes the R^2 values for different input combinations. The highest prediction accuracy for $COD_{effluent}$ (R^2 = 0.861) was achieved when all five parameters were included, indicating that both the influent quality and operational parameters play significant roles in COD removal. For NH_4-$N_{effluent}$ prediction, the best result (R^2 = 0.796) was observed when MLSS was excluded from the inputs, suggesting that ammonium removal may be more strongly influenced by influent characteristics than by the biomass concentration.

Table 17. R^2 values of ANN models using different input parameter combinations.

No	Input Parameters	R^2 (NH_4^+-$N_{MBReffluent}$)	R^2 ($COD_{MBReffluent}$)
1	$COD_{influent}$, NH_4^+-$N_{influent}$, $TSS_{influent}$, $Temperature_{influent}$, $MLSS_{MBR}$	0.610	0.861
2	$COD_{influent}$, NH_4^+-$N_{influent}$, $TSS_{influent}$, $Temperature_{influent}$	0.796	0.847
3	$COD_{influent}$, NH_4^+-$N_{influent}$, $TSS_{influent}$, $MLSS_{MBR}$	0.523	0.821
4	$COD_{influent}$, $TSS_{influent}$, $Temperature_{influent}$, $MLSS_{MBR}$	0.717	0.812
5	NH_4^+-$N_{influent}$, $TSS_{influent}$, $Temperature_{influent}$, $MLSS_{MBR}$	0.710	0.844
6	NH_4^+-$N_{influent}$, $Temperature_{influent}$, $MLSS_{MBR}$	0.735	0.847
7	$COD_{influent}$, NH_4^+-$N_{influent}$, $Temperature_{influent}$	0.736	0.800
8	$COD_{influent}$, NH_4^+-$N_{influent}$, $MLSS_{MBR}$	0.630	0.810
9	$TSS_{influent}$, $Temperature_{influent}$, $MLSS_{MBR}$	0.703	0.810
10	$COD_{influent}$, NH_4^+-$N_{influent}$	0.650	0.580

The overall results highlight the importance of multi-parameter inputs in achieving accurate predictions. The decrease in performance when fewer variables were used confirms the value of complex data structures in modeling biological treatment systems.

To further assess model performance, Table 18 presents the MSE values for the training, validation, and testing datasets across ten ANN models for $COD_{effluent}$. Most models showed low MSEs during training (0.0022–0.0035), indicating effective learning.

Table 18. MSE values of 10 ANN trials for $COD_{effluent}$ prediction.

No	Training	Validation	Test
1	0.0026	0.0017	0.0062
2	0.0026	0.0010	0.0050
3	0.0022	0.0082	0.0011
4	0.0031	0.0031	0.0064
5	0.0029	0.0027	0.0069
6	0.0031	0.0026	0.0054
7	0.0023	0.0017	0.0068
8	0.0027	0.0083	0.0099
9	0.0035	0.0037	0.0037
10	0.0069	0.0099	0.0013

Model 3 and Model 10 demonstrated the lowest test MSEs (0.0011 and 0.0013, respectively), suggesting strong generalization capability. Models 1 and 2 also displayed a balanced performance, making them reliable for stable COD predictions. In contrast, Model 8 showed the highest validation and test errors, indicating possible overfitting.

The correlation matrix of MSE values is presented in Figure 19. A weak correlation was observed between the training and validation datasets, while a moderate positive correlation was noted between the validation and test datasets. This indicates varying degrees of consistency in model generalization across trials.

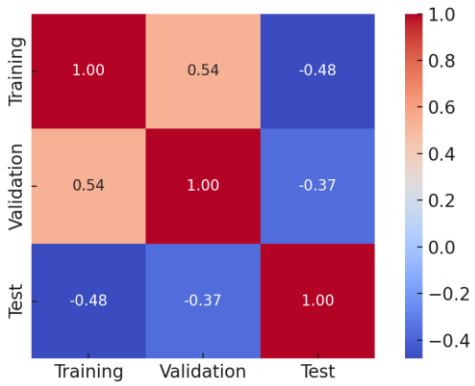


Figure 19. Correlation matrix of MSE values for $COD_{effluent}$ prediction.

Figure 20 illustrates the architecture of Model 1, comprising five input neurons ($COD_{influent}$, NH_4-$N_{influent}$, $SS_{influent}$, temperature, and MLSS), one hidden layer with 20 neurons, and one output neuron predicting $COD_{effluent}$.

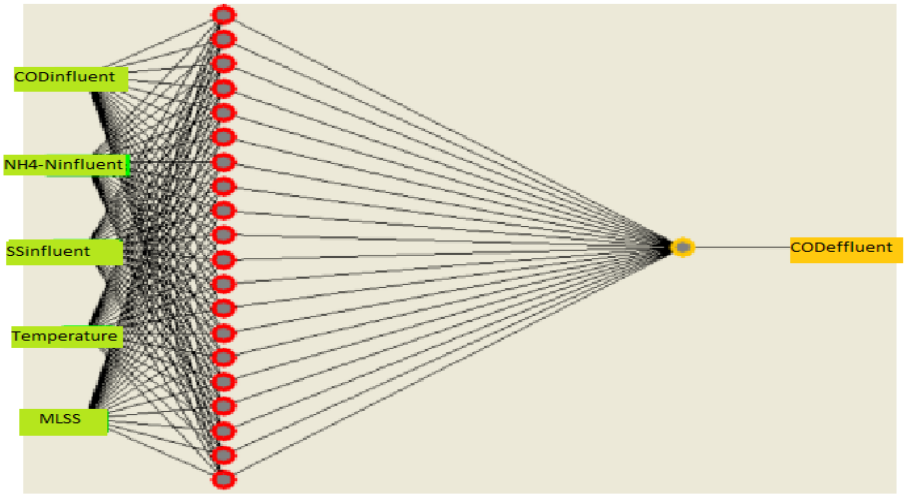


Figure 20. ANN Model No.1 architecture for COD prediction.

Table 19 summarizes the MSE values from 10 ANN trials aimed at predicting NH_4^+-N effluent concentrations. Trial 10 achieved the lowest test MSE (0.00104), indicating the best generalization capability, while Trial 5 exhibited the highest test MSE (0.00981), suggesting overfitting or suboptimal training.

Table 19. MSE values from 10 ANN trials for NH_4-Neffluent prediction.

Trial	Training	Validation	Test
1	0.00159	0.00162	0.00147
2	0.00102	0.00166	0.00723
3	0.00315	0.00322	0.00762
4	0.00233	0.00453	0.00401
5	0.00131	0.00309	0.00981
6	0.00179	0.00262	0.00532
7	0.00165	0.00241	0.00519
8	0.00205	0.00241	0.00529
9	0.00264	0.00196	0.00424
10	0.00123	0.00195	0.00104

These results confirm that while ANN models demonstrated a strong predictive capacity overall, certain configurations suffered from overfitting, highlighting the importance

of careful input selection, training–validation–test separation, and model architecture optimization.

Models with balanced MSE values across all phases (e.g., Trials 1 and 10) demonstrated a more stable performance. This highlights the sensitivity of ANN models to initial conditions and the importance of validation. The correlation matrix in Figure 21 showed a strong positive correlation ($r \approx 0.89$) between the training and validation phases, and moderate correlations between other phases. This suggests consistent model behavior across data splits.

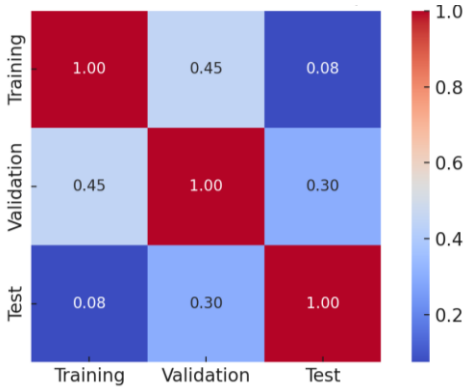


Figure 21. Correlation matrix of MSE values for NH_4-$N_{effluent}$ prediction.

Figure 22 shows the structure of Model 2, which was used for predicting NH_4-$N_{effluent}$. It includes four input neurons ($COD_{influent}$, NH_4-$N_{influent}$, $SS_{influent}$, temperature), a hidden layer with 20 neurons, and one output neuron.

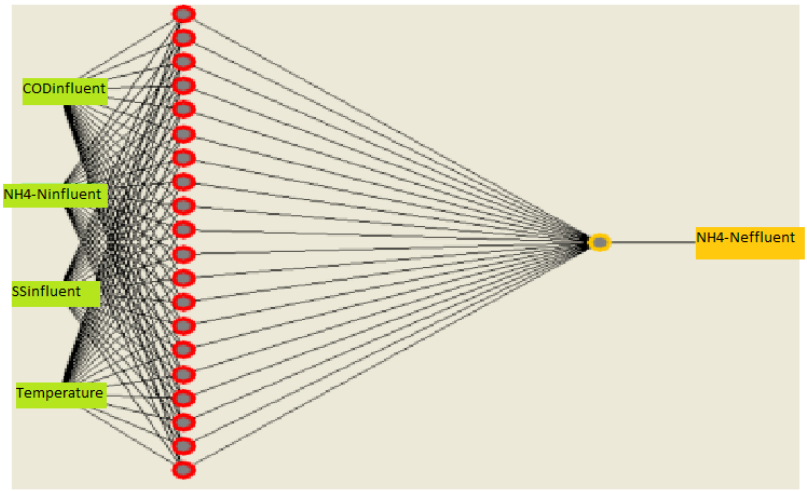


Figure 22. ANN Model No.2 architecture for NH_4-N prediction.

3.7.2. Principal Component Analysis (PCA) Results

PCA was applied to assess the contribution of input variables to the effluent COD and NH_4-N concentrations. Table 20 presents the PCA loadings for $COD_{effluent}$. Effluent COD was mainly associated with PC2, along with temperature. Influents such as COD and MLSS contributed to loading profiles but had a limited direct influence on effluent performance. Random Forest analysis further supported these findings with an R^2 of 0.359 and MSE of 0.334. A variable importance analysis showed that MLSS was the most dominant parameter, explaining 39% of the variance.

Table 20. PCA loadings for $COD_{effluent}$.

	PC1	PC2	PC3	PC4	PC5
$COD_{influent}$ (mg/L)	0.6035	0.0070	0.0794	−0.45688	0.6485
NH_4-$N_{influent}$ (mg/L)	0.4111	−0.1865	0.0090	0.8630	0.2263
$Temperature_{influent}$ (°C)	0.25623	0.4798	−0.8292	0.0232	−0.1256
MLSS (g/L)	0.6274	0.0363	0.3180	−0.1105	−0.7011
$COD_{effluent}$ (mg/L)	0.0856	−0.8564	−0.4524	−0.1833	−0.1441

Table 21 presents the PCA loadings for NH_4-$N_{effluent}$. PC1 was strongly associated with MLSS, $SS_{influent}$, and $COD_{influent}$. PC2 showed a positive correlation with NH_4-$N_{influent}$ and negative correlation with $COD_{influent}$. Random Forest modeling revealed that NH_4-$N_{effluent}$ had a strong prediction capacity, with R^2 = 0.804 and MSE = 0.87.

Table 21. PCA loadings for NH_4-$N_{effluent}$.

	PC1	PC2	PC3	PC4
$COD_{influent}$ (mg/L)	0.2895	−0.5119	−0.6908	−0.18800
NH_4-$N_{influent}$ (mg/L)	0.2812	0.7172	−0.0650	−0.4820
$SS_{influent}$ (g/L)	0.3447	0.3322	−0.2724	0.8267
$Temperature_{influent}$ (°C)	−0.5295	0.0731	−0.2621	0.0458
MLSS (g/L)	0.5430	−0.0097	−0.1013	−0.1950
NH_4-$N_{effluent}$ (mg/L)	−0.3780	0.3281	−0.6043	−0.0930

These results emphasize the nonlinear interactions among variables influencing ammonium removal, and the potential of machine learning techniques such as Random Forest and PCA in revealing such complex relationships.

ANN and PCA analyses proved effective in modeling and interpreting the behavior of MBR systems treating landfill leachate. Multi-variable input structures yielded better performance, and nonlinear methods captured subtle dependencies between influent conditions and effluent quality. The integration of ANN and PCA enhances the predictive capacity and provides actionable insights for optimizing system design and operation.

3.8. Evaluation of the Seasonal Effect on COD and NH_4-N Removal

ANOVA was applied to examine whether the seasonal COD and NH_4-N removals were significant or not, and a post hoc test (Tukey's HSD test) was applied to determine which seasons were effective. According to the ANOVA result, the seasonal differences in COD removal were statistically significant ($p < 0.001$). According to Tukey's HSD test, the season pairs with significant differences were winter–spring, summer–spring, and autumn–spring. Spring is the season with significantly higher COD removal compared to the other three seasons. In NH_4-N removal, according to the ANOVA result, there is a statistically significant difference between the removal rates according to the seasons ($p < 0.001$). Spring exhibited significantly higher removal efficiencies compared to winter and autumn ($p < 0.001$). When autumn and spring are compared, spring again provides higher removal (difference: +0.82%, $p < 0.001$) There is no statistically significant difference between the other seasons. Both NH_4-N and COD removal increased significantly in spring. This increase is probably due to the seasonal effects of temperature, microbial activity or operating conditions. In winter, the performance decreases; in particular, the deviation in NH_4-N removal is higher.

3.9. Model Validation Using RMSE and MAE Metrics

Model validation was performed to assess the predictive performance of the ANN models using RMSE and MAE metrics across the training, validation, and testing phases. These statistical measures provide insights into both the variance and the average magnitude of prediction errors.

Tables 22 and 23 present the RMSE and MAE values for COD and NH_4-N effluent predictions, respectively, including 95% confidence intervals (CI).

Table 22. Model validation results for $COD_{effluent}$ prediction.

Data Set	RMSE (mg/L)	MAE (mg/L)	95% CI (RMSE)	95% CI (MAE)
Model 1				
Training	0.051	0.063	0.051–0.107	0.040–0.086
Validation	0.041	0.033	0.026–0.055	0.021–0.045
Test	0.078	0.063	0.050–0.106	0.040–0.086
Model 2				
Training	0.051	0.057	0.045–0.107	0.037–0.077
Validation	0.032	0.025	0.020–0.042	0.016–0.034
Test	0.071	0.057	0.045–0.096	0.037–0.077

Table 23. Model validation results for NH_4-N effluent prediction.

Data Set	RMSE (mg/L)	MAE (mg/L)	95% CI (RMSE)	95% CI (MAE)
Model 1				
Training	0.039	0.032	0.025–0.054	0.020–0.043
Validation	0.040	0.032	0.025–0.054	0.020–0.043
Test	0.038	0.031	0.024–0.052	0.019–0.041
Model 2				
Training	0.032	0.026	0.020–0.043	0.016–0.034
Validation	0.041	0.033	0.026–0.055	0.020–0.044
Test	0.085	0.068	0.054–0.115	0.043–0.092

Model 2, which demonstrated superior generalization capacity, achieved RMSE values of 0.051, 0.031, and 0.070 mg/L for the training, validation, and testing phases of COD prediction, respectively. For NH_4-N prediction using Model 2, the RMSE values were 0.031, 0.040, and 0.085 mg/L for the same respective phases.

To complement RMSE, MAE values were calculated to better represent the average deviation from the observed data. For NH_4-N prediction, Model 2 had an MAE of 0.078 mg/L, while Model 1 achieved a lower MAE of 0.029 mg/L. This indicates that although Model 2 had a slightly lower RMSE in validation, Model 1 provided more accurate results in terms of absolute error.

The combined evaluation using RMSE and MAE confirms the suitability of the ANN models in predicting effluent COD and NH_4-N concentrations under varying operational conditions.

In particular, Trial 5 showed a relatively higher MSE in NH_4-N prediction. This may be attributed to the sensitivity of the ANN to initial weight settings, variability in training–validation–test splits, and the inherently fluctuating nature of ammonium concentrations due to seasonal and operational changes. Despite preprocessing efforts such as outlier removal and normalization, these fluctuations presented challenges for the learning process—especially in models where key features like MLSS and temperature were omitted or sub-optimally weighted.

These findings underscore the importance of feature selection, architecture tuning, and cross-validation strategies in developing reliable prediction models for dynamic wastewater treatment systems.

4. Discussion

This study provides strong evidence for the effectiveness of a full-scale hybrid MBR–NF system in the treatment of municipal landfill leachate. The MBR unit consistently delivered high COD and NH_4^+-N removal efficiencies (averaging 93.5% and 98.6%, respectively), confirming its suitability for high-strength wastewaters. The aerobic zone exhibited a positive correlation between dissolved oxygen levels and COD removal, consistent with previous reports on the importance of aerobic stability for organic degradation [46,47]. Seasonal variations revealed that spring conditions led to the highest removal efficiencies, likely due to enhanced microbial activity under moderate temperatures.

The NF unit contributed significantly to phosphorus polishing, with TP removal efficiencies above 95%, yet showed a fluctuating performance in TN and COD removal. These instabilities may stem from operational factors such as membrane fouling, pressure variations, or fluctuating feed characteristics—issues commonly reported in membrane systems operating under high organic and ionic loads [48,49].

ANN modeling proved effective in predicting effluent COD and ammonium concentrations, achieving R^2 values of 0.861 and 0.796, respectively. These findings are in line with those of Giwa et al. (2021) and Yao et al. (2022), who highlighted the utility of machine learning in capturing nonlinear relationships in wastewater systems [50,51]. The model's robustness was further validated through RMSE and MAE analyses, with 95% confidence intervals confirming predictive consistency across the training, validation, and test phases.

However, the ANN models also revealed some overfitting sensitivity, particularly in NH_4^+-N predictions, suggesting that further improvements in the training data volume, input feature selection, and cross-validation strategies are needed. Trial 5, for instance, exhibited a high test MSE despite reasonable training accuracy—underscoring the importance of careful model calibration.

The correlation and regression analyses confirmed that the COD and TP removal performances were strongly aligned, while TN removal, particularly by NF, exhibited weaker and less predictable associations. This indicates that nitrogen removal remains a challenge and may benefit from additional strategies, such as carbon supplementation for denitrification or the integration of advanced oxidation processes.

Overall, the hybrid system demonstrated a synergistic performance: MBR ensured biological degradation and ammonium removal, while NF served as a polishing stage for phosphorus and residual COD. This synergy, combined with AI-based prediction capabilities, positions hybrid membrane systems as promising solutions for sustainable leachate treatment. Future research should focus on real-time ANN integration with SCADA systems, membrane fouling monitoring, and the exploration of ensemble learning models such as Convolutional Neural Network–Genetic Algorithm (CNN–GA) or Long Short-Term Memory (LSTM)–ANN for dynamic process control [51]. Similar approaches using CNN–GA were applied in wastewater quality prediction by Behera et al. (2024), reporting significant accuracy improvements [52].

5. Conclusions

This study successfully demonstrated the technical feasibility and operational reliability of a full-scale hybrid MBR–NF system for the treatment of landfill leachate at the Istanbul–Şile Kömürcüoda facility. Over a 16-month monitoring period, the system consistently achieved high removal efficiencies for key pollutants, including COD, NH_4^+-N, and

TP. The MBR unit served as the primary biological treatment stage and enabled the stable removal of organic and nitrogenous compounds under favorable conditions. Meanwhile, the NF unit functioned effectively as a polishing step, particularly in enhancing phosphorus removal and improving final effluent quality.

The implementation of ANN models contributed to the predictive understanding of effluent COD and NH_4^+-N concentrations. These models demonstrated high performance metrics, including low RMSE and MAE values and narrow confidence intervals, confirming their potential as decision-support tools in dynamic treatment environments. However, the results also revealed that the model's performance was sensitive to the selection of input parameters and network configuration, highlighting the need for further refinement to reduce overfitting risks and improve generalization.

Furthermore, seasonal variability was found to influence treatment performance, with significantly higher removal efficiencies observed during the spring months. This finding underscores the importance of dynamic operational strategies in response to environmental changes.

Overall, this study reinforces the value of integrating advanced membrane technologies with data-driven modeling approaches for effective leachate treatment. Future research should focus on the real-time integration of ANN models within SCADA systems, the inclusion of trace pollutants and membrane fouling indicators in predictive frameworks, and the optimization of NF membranes through surface modifications and adaptive process control. Such strategies will enhance system resilience, promote sustainable operation, and contribute to intelligent landfill leachate management.

Author Contributions: Conceptualization, E.Ç., V.B. and S.G.-D.; methodology, E.Ç. and V.B.; software, V.B.; validation, E.Ç., V.B. and S.G.-D.; formal analysis, E.Ç., V.B. and S.G.-D.; investigation, E.Ç. and V.B.; resources, E.Ç., V.B. and S.G.-D.; data curation, E.Ç., V.B. and S.G.-D.; writing—original draft preparation, E.Ç., V.B. and S.G.-D.; writing—review and editing, S.G.-D.; visualization, E.Ç. and S.G.-D.; supervision, E.Ç.; project administration, E.Ç.; funding acquisition, E.Ç. and V.B. All authors have read and agreed to the published version of the manuscript.

Funding: This research received no external funding.

Data Availability Statement: The raw data supporting the conclusions of this article will be made available by the authors on request.

Conflicts of Interest: Author Vahit Balahorlu was employed by the company IZAYDAS. The remaining authors declare that the research was conducted in the absence of any commercial or financial relationships that could be construed as a potential conflict of interest.

Abbreviations

The following abbreviations are used in this manuscript:

MBR	Membrane Bioreactor
NF	Nanofiltration
UF	Ultrafiltration
RO	Reverse Osmosis
AI	Artificial Intelligence
ANN	Artificial Neural Network
TiO_2	Titanium Dioxide
COD	Chemical Oxygen Demand
TSS	Total Suspended Solids
MLSS	Mixed Liquor Suspended Solids
TKN	Total Kjeldahl Nitrogen
OLS	Ordinary Least Squares

MSE	Mean Squared Error
TDS	Total Dissolved Solids
CNN	Convolutional Neural Network
GRNNs	General Regression Neural Networks
CNN-LSTM	Convolutional Neural Network–Long Short-Term Memory
CIP	Clean-In-Place
MSE	Mean Squared Error
RMSE	Root Mean Squared Error
MAE	Mean Absolute Error
PCA	Principal Component Analysis

References

1. Guo, Y.; Li, P.; He, X.; Wang, L. Groundwater Quality in and Around a Landfill in Northwest China: Characteristic Pollutant Identification, Health Risk Assessment, and Controlling Factor Analysis. *Expo. Health* **2022**, *14*, 885–901. [CrossRef]
2. Gupta, S.; Raju, N.J. Potential Environmental Pollution Study by Leachate Generation and Health Risk Assessment in the Vicinity of Bandhwari Landfill Disposal Site, National Capital Region, India. *Groundw. Sustain. Dev.* **2023**, *23*, 101032. [CrossRef]
3. Oumaima, E.B.; Cano, Á.F.; Avilés, J.; Fechtali, T. Characterization of Leachate from Different Landfills Sites of Morocco and Spain: A Comparative Study. *Eur. Sci. J. ESJ* **2019**, *15*, 183–190. [CrossRef]
4. Manea, E.E.; Bumbac, C. Sludge Composting—Is This a Viable Solution for Wastewater Sludge Management? *Water* **2024**, *16*, 2241. [CrossRef]
5. Ilmasari, D.; Kamyab, H.; Yuzir, A.; Riyadi, F.; Khademi, T.; Al-Qaim, F.; Kirpichnikova, I.; Krishnan, S. A Review of the Biological Treatment of Leachate: Available Technologies and Future Requirements for the Circular Economy Implementation. *Biochem. Eng. J.* **2022**, *187*, 108605. [CrossRef]
6. Wei, M.; Zhang, R.; Zhou, M.; Yuan, Z.; Yuan, H.; Zhu, N. Treatment of Fresh Leachate by Microaeration Pretreatment Combined with IC-AO2 Process: Performance and Mechanistic Insight. *Sci. Total Environ.* **2021**, *789*, 147939. [CrossRef]
7. Zisman, O.; Kushmaro, A.; Brenner, A. Bio-Chemical Treatment of Landfill Leachates with High Load of Organic and Nitrogen Compounds. *Sustain. Chem. Environ.* **2024**, *5*, 100061. [CrossRef]
8. Farsani, M.H.; Yengejeh, R.J.; Mirzahosseini, A.H.; Monavari, M.; Hassani, A.h.; Mengelizadeh, N. Effective Leachate Treatment by a Pilot-Scale Submerged Electro-Membrane Bioreactor. *Environ. Sci. Pollut. Res.* **2021**, *29*, 9218–9231. [CrossRef]
9. Yekani, N.H.; Peyravi, M.; Jahanshahi, M.; Bagheri, M. Design and Annual Operation of Full Scale Landfill Leachate Plant in Iran: Focus on Multistage Membrane Technology. *Chem. Pap.* **2022**, *76*, 4509–4521. [CrossRef]
10. Brancato, S.M.; Salzano, D.; Lellis, F.D.; Fiore, D.; Russo, G.; Bernardo, M. In Vivo Learning-Based Control of Microbial Populations Density in Bioreactors. In Proceedings of the 6th Annual Learning for Dynamics & Control Conference, Oxford, UK, 15–17 July 2023.
11. Liu, S.; Foo, Z.H.; Lienhard, J.H.; Keten, S.; Lueptow, R.M. Membrane Charge Effects on Solute Transport in Polyamide Membranes. *arXiv* **2025**, arXiv:2503.10871.
12. Molina, M.; Ribeiro, R.P.; Veloso, B.; Gama, J. Super-Resolution Analysis for Landfill Waste Classification. In Proceedings of the International Symposium on Intelligent Data Analysis, Stockholm, Sweden, 24–26 April 2024.
13. de Almeida, R.; de Souza Couto, J.M.; Gouvea, R.M.; de Almeida Oroski, F.; Bila, D.; Quintaes, B.R.; Campos, J. Nanofiltration Applied to the Landfill Leachate Treatment and Preliminary Cost Estimation. *Waste Manag. Res.* **2020**, *38*, 1119–1128. [CrossRef]
14. Reis, B.G.; Silveira, A.L.; Lebron, Y.; Moreira, V.R.; Teixeira, L.; Okuma, A.; Amaral, M.; Lange, L. Comprehensive Investigation of Landfill Leachate Treatment by Integrated Fenton/Microfiltration and Aerobic Membrane Bioreactor with Nanofiltration. *Process Saf. Environ. Prot.* **2020**, *143*, 121–128. [CrossRef]
15. Liu, G.; Han, M.; Luo, W.; Liu, Y.; Fang, J.; Tian, M.; Wang, L.; Zhao, S.; Meng, F. Loose Nanofiltration—Membrane Distillation Integrated Process for Resource Recovery from Leachate MBR Effluent: Performance and Membrane Fouling. *Desalination* **2023**, *545*, 116185. [CrossRef]
16. Kim, J.; Wu, B.; Jeong, S.; Jeong, S.; Kim, M. Recent Advances of Membrane-Based Hybrid Membrane Bioreactors for Wastewater Reclamation. *Front. Membr. Sci. Technol.* **2024**, *3*, 1361433. [CrossRef]
17. Rall, D.; Schweidtmann, A.M.; Krusea, M.; Evdochenko, E.; Mitsos, A.; Wessling, M. Multi-Scale Membrane Process Optimization with High-Fidelity Ion Transport Models through Machine Learning. *J. Membr. Sci.* **2020**, *608*, 118208. [CrossRef]
18. Ling, B.; Battiato, I. Rough or Wiggly? Membrane Topology and Morphology for Fouling Control. *J. Fluid Mech.* **2019**, *862*, 753–780. [CrossRef]

19. Igwegbe, C.A.; Onyechi, C.C.; Białowiec, A.; Onukwuli, O. Enhancing Municipal Solid Waste Leachate Treatment Efficiency: AI-Based Prediction of Electrocoagulation/Flocculation Recovery Using Iron Electrodes. *Environ. Technol.* **2024**, *45*, 6184–6199. [CrossRef]
20. Desai, N.; Soraganvi, V.S.; Madabhavi, V.K. Solar Photocatalytic Degradation of Organic Contaminants in Landfill Leachate Using TiO2 Nanoparticles by RSM and ANN. *Nat. Environ. Pollut. Technol.* **2020**, *19*, 651–662. [CrossRef]
21. Matovelle, C.; Quinteros, M.; Heras, D. Machine Learning Techniques in Dosing Coagulants and Biopolymers for Treating Leachate Generated in Landfills. *Water* **2023**, *15*, 4200. [CrossRef]
22. Singa, P.; Isa, M.; Sivaprakash, B.; Ho, Y.; Lim, J.-W.; Rajamohan, N. PAHs Remediation from Hazardous Waste Landfill Leachate Using Fenton, Photo—Fenton and Electro—Fenton Oxidation Processes—Performance Evaluation under Optimized Conditions Using RSM and ANN. *Environ. Res.* **2023**, *231*, 116191. [CrossRef]
23. Tchobanoglous, G.; Theisen, H.; Vigil, S.A. *Integrated Solid Waste Management: Engineering Principles and Management Issues*; McGraw-Hill: New York, NY, USA, 1993; ISBN 978-0-07-112865-0.
24. American Public Health Association. *Standard Methods for the Examination of Water and Wastewater*, 19th ed.; APHA: Washington, DC, USA, 1995.
25. Elfilali, N.; Essafi, N.; Zait, M.; Tahaikt, M.; Elazhar, F.; Elmidaoui, A.; Taky, M. Effectiveness of Membrane Bioreactor/Reverse Osmosis Hybrid Process for Advanced Purification of Landfill Leachate. *Dasalination Water Treat.* **2021**, *240*, 24–32. [CrossRef]
26. Hamedi, H.; Mohammadzadeh, O.; Rasouli, S.; Zendehboudi, S. A Critical Review of Biomass Kinetics and Membrane Filtration Models for Membrane Bioreactor Systems. *J. Environ. Chem. Eng.* **2021**, *9*, 106406. [CrossRef]
27. Jha, S.; Mishra, B.K. An Overview of Deploying Different Treatment Processes with Membrane Bioreactor for Enhanced Treatment of Wastewaters: Synergistic Performances and Reduced Fouling of Membrane. *Environ. Sci. Pollut. Res. Int.* **2024**, *31*, 63603–63634. [CrossRef]
28. Rahman, T.; Roy, H.; Islam, M.R.; Tahmid, M.; Fariha, A.; Mazumder, A.; Tasnim, N.; Pervez, M.; Cai, Y.; Naddeo, V.; et al. The Advancement in Membrane Bioreactor (MBR) Technology toward Sustainable Industrial Wastewater Management. *Membranes* **2023**, *13*, 181. [CrossRef]
29. Badr, E.; Gzar, H. Evaluating Laboratory Side-Stream Membrane Bioreactor and Nanofiltration System for Treating Domestic Wastewater and Reuse. *Wasit J. Eng. Sci.* **2022**, *10*, 234–243. [CrossRef]
30. Wongburi, P.; Park, J.K. Prediction of Wastewater Treatment Plant Effluent Water Quality Using Recurrent Neural Network (RNN) Models. *Water* **2023**, *15*, 3325. [CrossRef]
31. Bland, C.; Tonello, L.; Biganzoli, E.; Snowdon, D.; Antuono, P.; Lanza, M. *Advances in Artificial Neural Networks*; Academic Archive in Biomedical & Life Sciences: Bejing, China, 2020.
32. Lai, K.C.; Lim, S.; Teh, P.; Yeap, K. Modeling Electrostatic Separation Process Using Artificial Neural Network (ANN). *Procedia Comput. Sci.* **2016**, *91*, 372–381. [CrossRef]
33. Pekel, E.; Gul, M.; Celik, E.; Yousefi, S. Metaheuristic Approaches Integrated with ANN in Forecasting Daily Emergency Department Visits. *Math. Probl. Eng.* **2021**, *2021*, 9990906. [CrossRef]
34. Touzani, A.; Hammoudani, Y.E.; Dimane, F.; Tahiri, M.; Haboubi, K. Characterization of Leachate and Assessment of the Leachate Pollution Index—A Study of the Controlled Landfill in Fez. *Ecol. Eng. Environ. Technol.* **2024**, *25*, 57–69. [CrossRef]
35. Turki, N.; Boujelben, N.; Bakari, Z.; Kettab, A.; Bouzid, J. Removal of Organic and Nitrogen Compounds from Landfill Leachates by Coagulation, Fenton and Adsorption Coupling Processes. *Desalination Water Treat.* **2021**, *213*, 279–287. [CrossRef]
36. Murhunzi, B.A.; Olukanni, D.O.; Oyegbile, B.A. Sustainable Approach of Biological Treatment of Landfill Leachate by Anaerobic Ammonium Oxidation: A Review. *IOP Conf. Ser. Earth Environ. Sci.* **2024**, *1342*, 012039. [CrossRef]
37. Farhangi, M.; Ghasemzadeh, Z.; Ghorbanzadeh, N.; Khalilirad, M.; Unc, A. Phosphate Removal from Landfill Leachate Using Ferric Iron Bioremediation under Anaerobic Condition. *J. Mater. Cycles Waste Manag.* **2021**, *23*, 1576–1587. [CrossRef]
38. Waara, S.; Wojciechowska, E. Treatment of Landfill Leachate in a Constructed Free Water Surface Wetland System over a Decade—Identification of Disturbance in Process Behaviour and Removal of Eutrophying Substances and Organic Material. *J. Environ. Manag.* **2019**, *249*, 109319. [CrossRef]
39. Hanafiah, M.; Aziz, N.I.H.A.; Halim, A.A.; Shamdin, L.S.; Razzak, L. Phytoremediation of Landfill Leachate Using Ipomoea Aquatica and Pistia Stratiotes. *J. Environ. Biol.* **2021**, *42*, 775–781. [CrossRef]
40. Ramli, S.F.; Aziz, H.A.; Omar, F.M.; Yusoff, M.; Halim, H.; Kamaruddin, M.A.; Ariffin, K.S. Removal of Colour and Suspended Solids from Landfill Leachate Using Tin Tetrachloride (SnCl4): The Effects of pH, Zeta Potential, and Particle Sizes. *Int. J. Environ. Anal. Chem.* **2021**, *103*, 6294–6309. [CrossRef]
41. Li, X.; Lu, M.-Y.; Huang, Y.; Yuan, Y.; Yuan, Y. Influence of Seasonal Temperature Change on Autotrophic Nitrogen Removal for Mature Landfill Leachate Treatment with High-Ammonia by Partial Nitrification-Anammox Process. *J. Environ. Sci.* **2021**, *102*, 291–300. [CrossRef]
42. Mieczkowski, D.; Cydzik-Kwiatkowska, A.; Rusanowska, P.; Świątczak, P. Temperature-Induced Changes in Treatment Efficiency and Microbial Structure of Aerobic Granules Treating Landfill Leachate. *World J. Microbiol. Biotechnol.* **2016**, *32*, 91. [CrossRef]

43. Coulibaly, Y.; Koné, T.; Kamagaté, M.; Ouattara, J.; Coulibaly, S.; Coulibaly, L. Characterization of the Leachate from the Municipal Landfill of Akouédo (Abidjan, Côte d´Ivoire). *J. Environ. Earth Sci.* **2020**, *10*, 17–22. [CrossRef]
44. Li, W.; Sun, Y.; Bian, R.; Wang, H.; Zhang, D. N2O Emissions from an Intermittently Aerated Semi-Aerobic Aged Refuse Bioreactor: Combined Effect of COD and NH4+-N in Influent Leachate. *Waste Manag.* **2017**, *69*, 242–249. [CrossRef]
45. Song, F.; Ban, C.; Xu, L.; Cao, W.; Zhang, Y. Treatment of COD and Ammonia Removal in Initial Landfill Leachate by an Aerobic SBR System. *Environ. Sci. Technol.* **2012**, *35*, 110–113.
46. Shahouni, R.; Abbasi, M.; Dibaj, M.; Akrami, M. Utilising Artificial Intelligence to Predict Membrane Behaviour in Water Purification and Desalination. *Water* **2024**, *16*, 2940. [CrossRef]
47. Ibrahim, M.; Haider, A.; Lim, J.W.; Mainali, B.; Aslam, M.; Kumar, M.; Shahid, M.K. Artificial Neural Network Modeling for the Prediction, Estimation, and Treatment of Diverse Wastewaters: A Comprehensive Review and Future Perspective. *Chemosphere* **2024**, *362*, 142860. [CrossRef] [PubMed]
48. Jia, T.-Z.; Rong, M.-Y.; Chen, C.-T.; Yong, W.F.; Lau, S.K.; Zhou, R.-F.; Chen, M.; Sun, S.-P. Recent Advances in Nanofiltration-Based Hybrid Processes. *Desalination* **2023**, *565*, 116852. [CrossRef]
49. Khoiruddin, K.; Boopathy, R.; Kawi, S.; Wenten, I.G. Towards Next-Generation Membrane Bioreactors: Innovations, Challenges, and Future Directions. *Curr. Pollut. Rep.* **2025**, *11*, 15. [CrossRef]
50. Giwa, A.; Yusuf, A.; Balogun, H.A.; Sambudi, N.S.; Bilad, M.R.; Adeyemi, I.; Chakraborty, S.; Curcio, S. Recent Advances in Advanced Oxidation Processes for Removal of Contaminants from Water: A Comprehensive Review. *Process Saf. Environ. Prot.* **2021**, *146*, 220–256. [CrossRef]
51. Yao, J.; Wu, Z.; Liu, Y.; Zheng, X.; Zhang, H.; Dong, R.; Qiao, W. Predicting Membrane Fouling in a High Solid AnMBR Treating OFMSW Leachate through a Genetic Algorithm and the Optimization of a BP Neural Network Model. *J. Environ. Manag.* **2022**, *307*, 114585. [CrossRef]
52. Behera, A.; Sahoo, K.S.; Mishra, T.K.; Bhuyan, M. A Combination Learning Framework to Uncover Cyber Attacks in IoT Networks. *Internet Things* **2024**, *28*, 101395. [CrossRef]

Disclaimer/Publisher's Note: The statements, opinions and data contained in all publications are solely those of the individual author(s) and contributor(s) and not of MDPI and/or the editor(s). MDPI and/or the editor(s) disclaim responsibility for any injury to people or property resulting from any ideas, methods, instructions or products referred to in the content.